

# Spacecraft Common Deployable Boom Hinge Deploy and Latching Mechanisms

Paul Lytal\* and Marcel Renson\*\*

## Abstract

JPL is developing deployable radio frequency (RF) reflector booms for spaceflight usage on two different earth orbiter projects scheduled to launch in the early 2020's. The static alignment and thermal stability requirements for these RF reflector booms are challenging. A common mechanism design has been developed for the deployment and latching of boom hinges which avoids significant parasitic loads on the alignment critical structures after completion of mechanism function. The mechanism design includes a high-aspect ratio torsion spring with viscous damper for hinge closure as well as an actuator-driven flexured hook and roller latch for joint preloading. This paper describes noteworthy mechanism design details, test results, challenges, and lessons learned during the development effort.

## Introduction

The RF reflector boom deployment sequence is shown in Figure 1 for each project. On a given boom, only one hinge is deployed and then latched at a time. After completion of hinge closure and latching for all boom hinges, the passive RF reflector deploys.

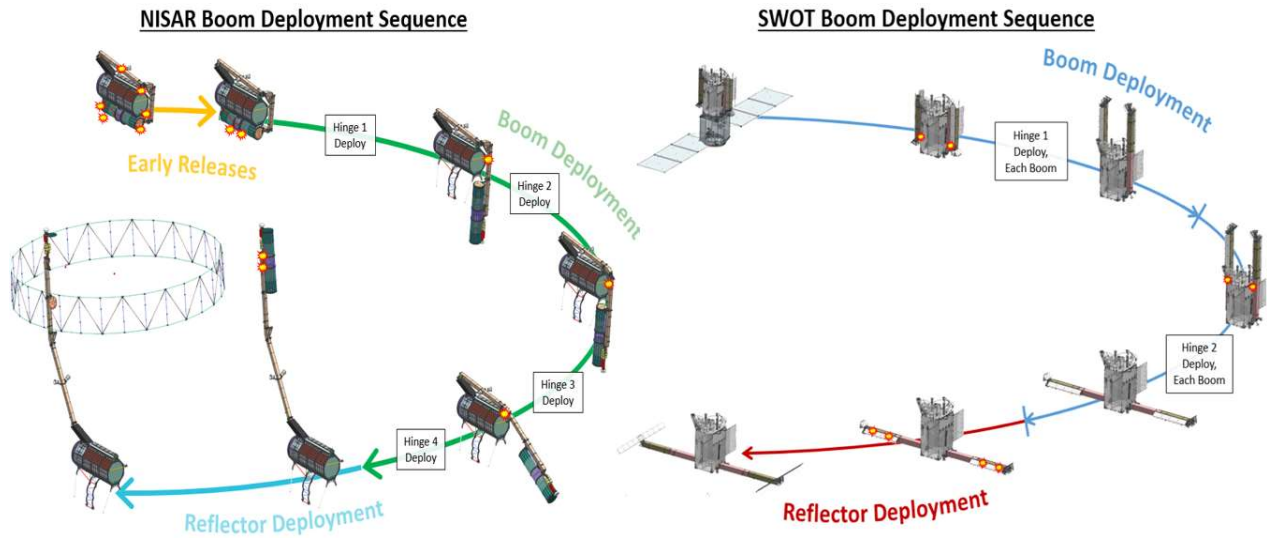


Figure 1. RF Reflector Boom Deployment Sequences

The boom hinge deploy and latching mechanism design includes a spring/damper mechanism for hinge closure and an actuator driven latching mechanism for hinge joint preloading (Figure 2). The spring/damper mechanism automatically proceeds with hinge closure immediately following mast launch restraint separation. Hinge latching does not commence until successful confirmation of hinge closure to within the latching capture range from redundant hinge closure sensors.

\* Jet Propulsion Laboratory, California Institute of Technology, Pasadena, CA

\*\* D.E.B. Manufacturing Inc., Lakewood, NJ

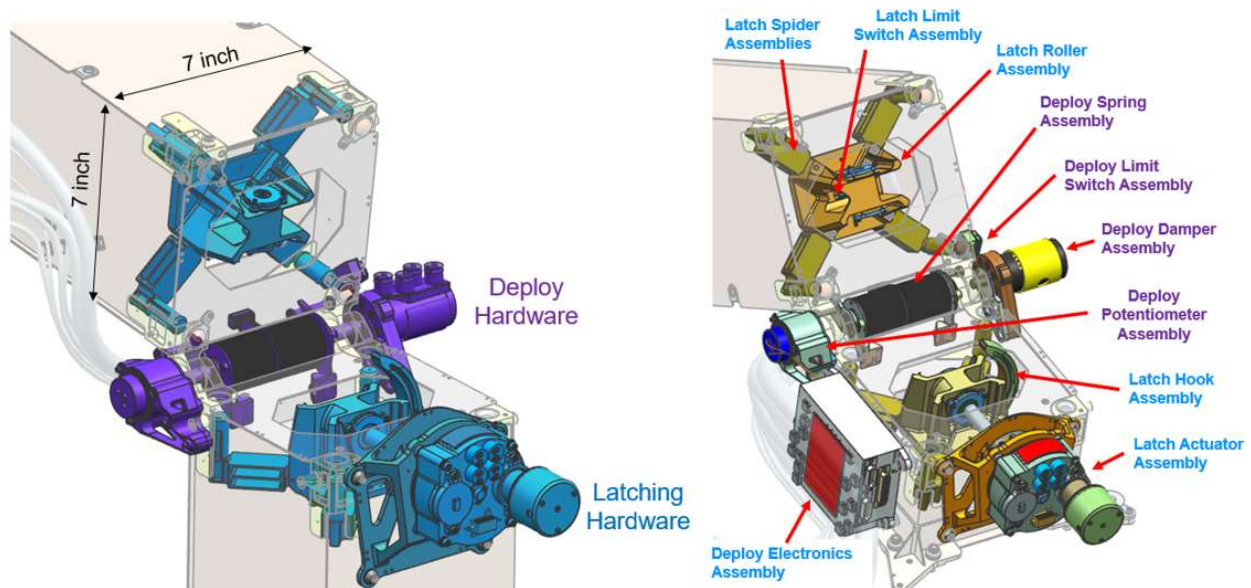


Figure 2. Hinge Deploy & Latching Mechanisms (NISAR Hinge Shown)

### Project Background

This common boom hinge deploy and latching mechanism design is being developed for two different earth-orbiter Projects: the Surface Water Ocean Topography (SWOT) Project and the NASA-ISRO Synthetic Aperture Radar (NISAR) Project. The SWOT Project is an international collaborative effort between NASA and the French Government Space Agency (CNES). The earth science objectives of the SWOT Project include high-definition temporal and spatial mapping of all fresh and salt water bodies around the globe for a minimum 42 month time period. NISAR is an international collaborative effort between NASA and the India Space Research Organization (ISRO). The earth science objectives of the NISAR Project include land and ice mass observation in order to improve natural disaster prediction, deforestation modeling, and polar ice cap reduction modeling amongst other objectives. Precision alignment and stability of the RF reflectors to the RF feeds is crucial to mission success of each project.

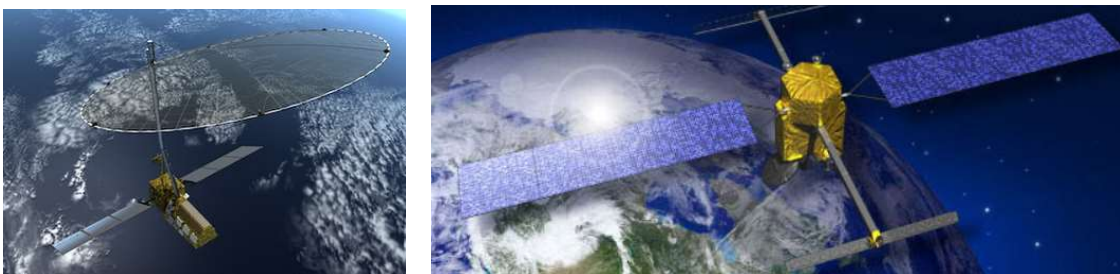


Figure 3. NISAR (Left) and SWOT (Right) Earth Observation Spacecraft

### Common Boom Deploy & Latching Mechanism Development

The SWOT and NISAR Projects elected to pursue a common deployable boom design to the maximum extent practical to reduce overall development cost and schedule. While detailed mast geometry

necessarily differs due to mission architecture and configuration differences, the basic design and construction of the booms is common between Projects.

The deploy and latching mechanisms are highly similar between projects, only differing as required by the structure that the mechanisms mount to and differences in flight environments. Noteworthy differences between Projects are highlighted in the sections that follow as relevant to the mechanisms described in this document.

### Driving Design Considerations

In addition to typical spaceflight mechanism design constraints (limited mass and volume, launch environments, on-orbit environments, ground testing considerations), the avoidance of significant and variable loading from mechanisms hardware onto the alignment critical structure was a primary design driver. The approach taken was to mechanically disconnect all possible mechanisms hardware from the mast after completion of mechanism function as show in Figure 4. In addition, the mechanical attachment of all mechanisms hardware to the mast uses flexures or non-preloaded pin/slot interfaces. Specific implementation of the mechanism mechanical decoupling is shown in Figure 5.

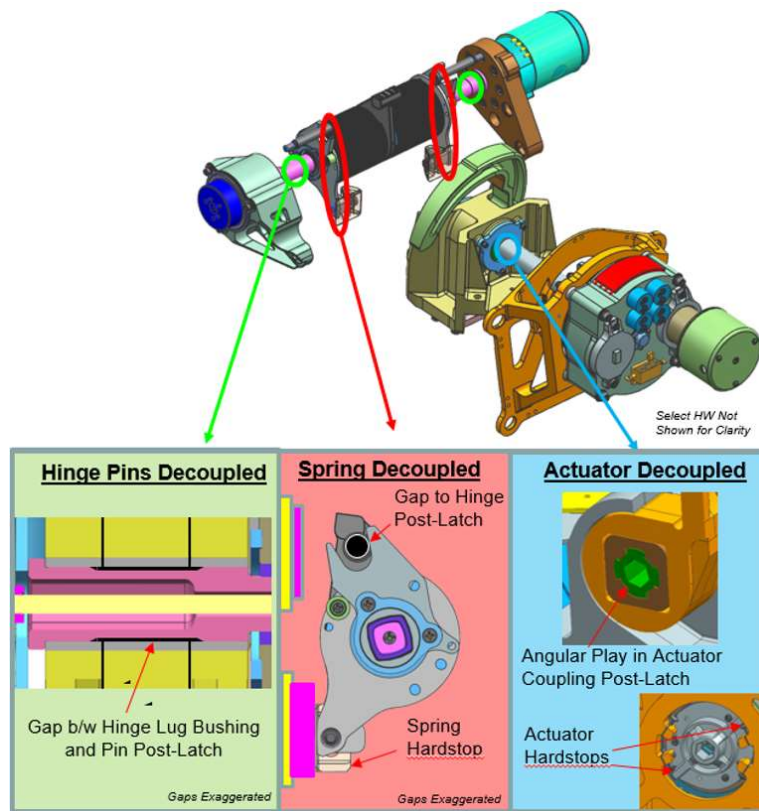


Figure 4. Mechanism Mechanical Disconnection from Alignment Critical Mast Structure

Another critical design driver for deploy and latching mechanisms hardware was conductive thermal isolation of mechanisms hardware from the mast structure. This enables the control of mechanism hardware to tighter temperature ranges than the parent structure as necessary. Isolation was accomplished using small contact areas and low thermal conductivity Ultem 2300 isolators. An example of this methodology is shown in Figure 5.

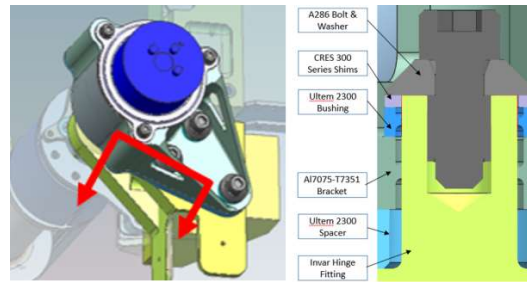


Figure 5. Example of SWOT and NISAR Mechanism Thermal Isolation Design

### Hinge Deployment Mechanism

The hinge deployment mechanism is designed to close boom hinges from launch stowed through deployed/closed hinge configuration. A separate analogous hinge deployment mechanism is used at each hinge. The hinge deployment mechanism was designed to overcome worst-case torque opposing deployment associated with hinge-crossing wire harness, coulomb friction sources, and ball bearing rolling friction losses over the full range of thermal environments deployment could take place in flight. Challenges encountered in the course of prototype hinge testing (Figure 6) in worst case thermal environments are described in the sections that follow.

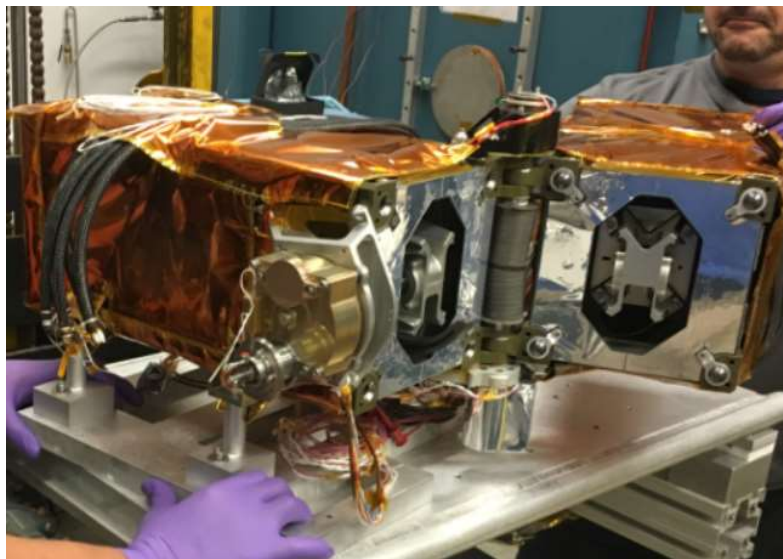


Figure 6. NISAR Prototype Thermal Test Hinge

A spring/damper mechanism was developed to perform hinge closure. Several different options were considered for the boom hinge closure mechanism. A serpentine wire rope spooler mechanism (as used on the SMAP Project RF boom) was considered but rejected primarily due to the inability to test mechanisms in a flight-like manner prior to full mast assembly. Various actuator-driven linkages were considered and discarded due to higher estimated mass than the spring/damper mechanism option. Direct actuator driven hinge closure was considered as well, but was also deemed more massive and a higher risk development than the spring/damper option.

The following sections provide information regarding unique design and testing challenges with the spring/damper mechanism as well as the deployable hinge crossing harness.

## Spring Design Overview

A pair of torsion springs is used at each hinge, each capable of independently transmitting torque to deploy the hinge for robustness. Each spring is supported by an aluminum outer mandrel which in-turn rotates on glass-filled Teflon bushings on an inner mandrel (Figure 7).

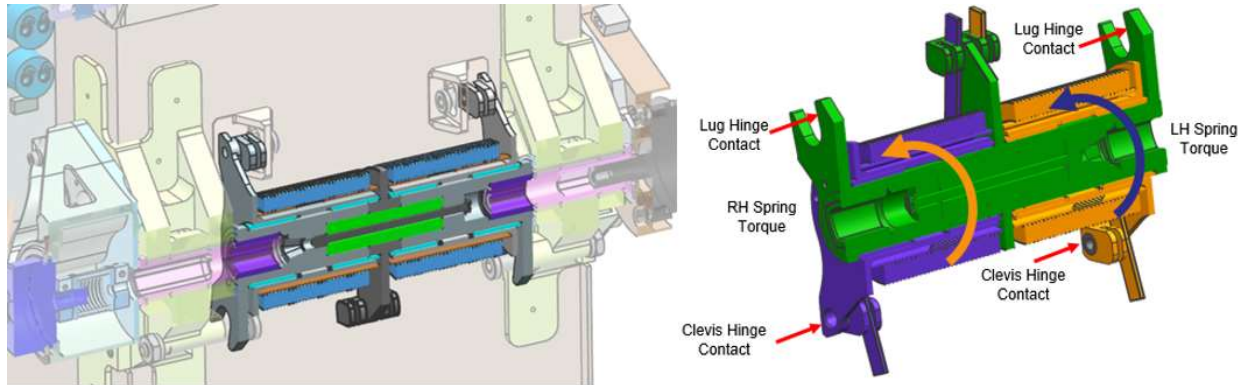


*Figure 7. Spring Location in Hinge (Left) and Independent Spring Mandrels (Right)*

A custom 17-7 CH900 torsion spring solution was deemed necessary given the limited volume and high output torque needed for the Hinge Deployment mechanism, particularly for the smaller volume available in the NISAR hinge configuration (116 mm [4.567 in] length and 43 mm [1.693 in] diameter for spring assembly). Elgiloy was briefly considered and dismissed due to long lead time as well as spring vendor cautionary guidance that Elgiloy spring development programs frequently encounter challenges often with little to no improvement in measured strength performance over 17-7 CH900. The Project elected to stick with the 17-7 CH900 material which the spring vendor has the most experience working with.

A high aspect ratio rectangular cross section (3.8 to 1) is being used for the spring to increase the spring wire moment of inertia per unit spring body length. This resulted in lower bending stress and higher spring constant than a round wire spring with the same wire width and number of spring turns.

There are six types of hinges for the SWOT and NISAR booms with different stow angles. It is worth noting that the relaxed spring arm angle for the springs for each hinge were selected to ensure maximum torque across the range of motion of the hinge without violating NASA-STD-5017A advisory that Mission Critical Springs maintain positive margins above a 1.5 factor of safety to yield in the maximum deflection (fully stowed) configuration [1].

## Spring Arm Twist

In early testing with spring arms contacting round pins with no other support, undesirable arm longitudinal twisting was observed at spring windup angles greater than 180 degrees, resulting in significant reduction in spring stiffness and higher-than-intended stress in the spring arms. Destructive characterization testing at room temperature demonstrated the onset of yielding at approximately 445 degrees as opposed to approximately 730 degrees predicted by analysis with no spring arm twist. Guide vanes were added to the spring mandrel design to minimize this arm twist phenomenon. Follow-on destructive spring testing demonstrated onset of yielding at approximately 740 degrees, which more closely matches analytical predictions (Figure 8).

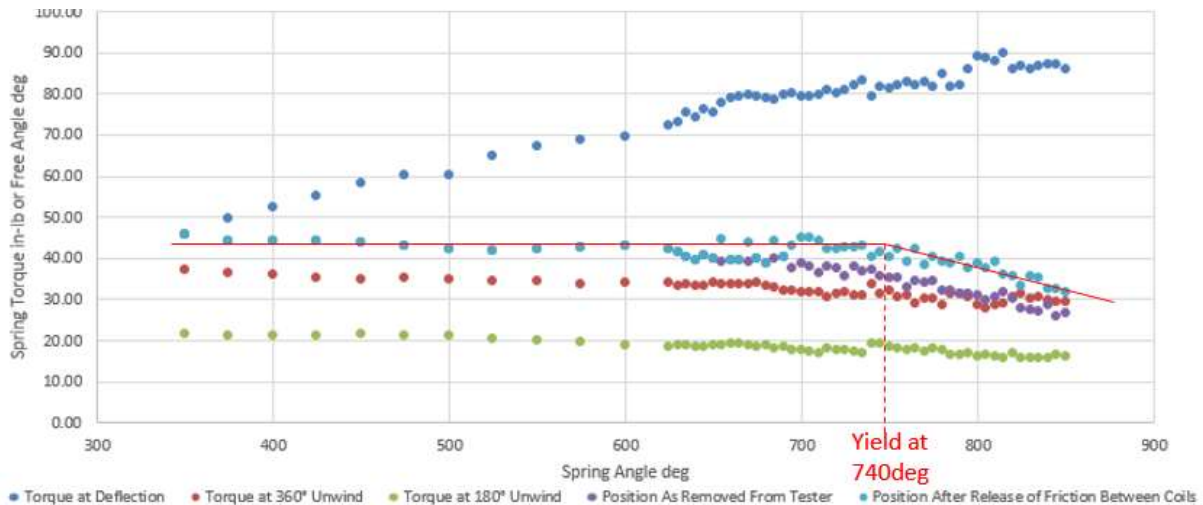


Figure 8. Destructive Spring Characterization Test Results, Spring Arms Supported

### Spring Assembly Thermal Testing

Developmental testing was conducted to evaluate the impact of spring wet lubrication on spring performance across temperature. Torsion springs were grease plated with a thin film of Braycote 601EF and tested in the same configuration as identical clean, unlubricated springs. Test results indicated that lubricated spring performance was nearly identical to unlubricated spring performance at and above room temperature. Unlubricated spring torque performance was significantly better than lubricated spring performance in the worst case cold environment (-100°C) as shown in Figure 9. The average improvement in spring output torque was up to 1.7 N·m [15 in·lbf] at maximum spring deflection in usage. This is expected to be the result of wet lubricant thickening at cold temperature. The flight torsion springs are unlubricated for both Projects.

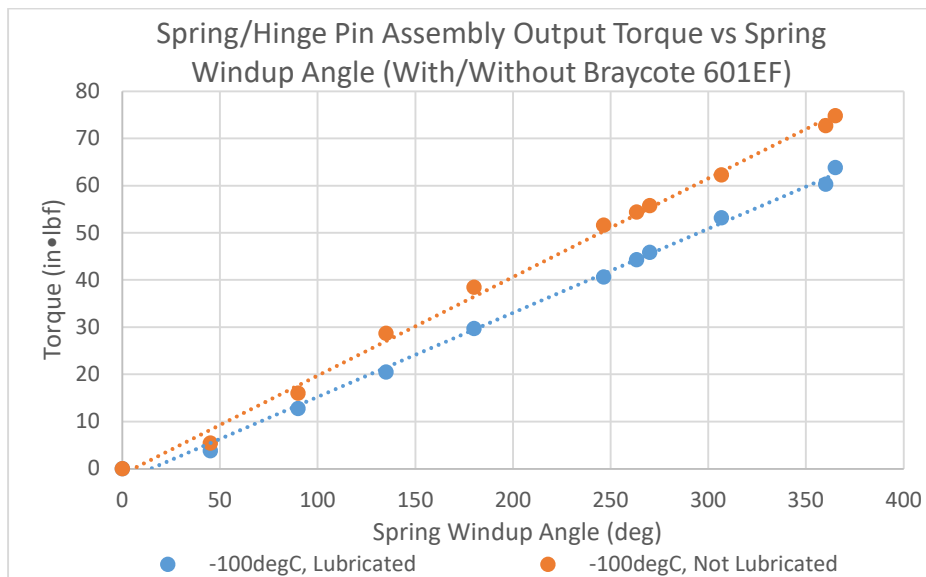


Figure 9. Prototype Spring Assembly Thermal Test, Lubricated versus Not Lubricated

Prototype spring assembly testing was also conducted at the hot and cold extremes of the expected flight operational temperature range. Test results demonstrate negligible change in spring/hinge pin assembly performance from 20°C to -100°C as shown in Figure 10. This is consistent with design expectations, as no wet lubricants are used in the spring assembly design and adequate clearance has been incorporated between all materials with dissimilar coefficients of thermal expansion internal to the mechanism. Furthermore, the flexural modulus of 17-7 CH900 springs changes negligibly from 20°C to -100°C. Similar results were observed between room temperature and the maximum flight design temperature for both Projects (+105°C).

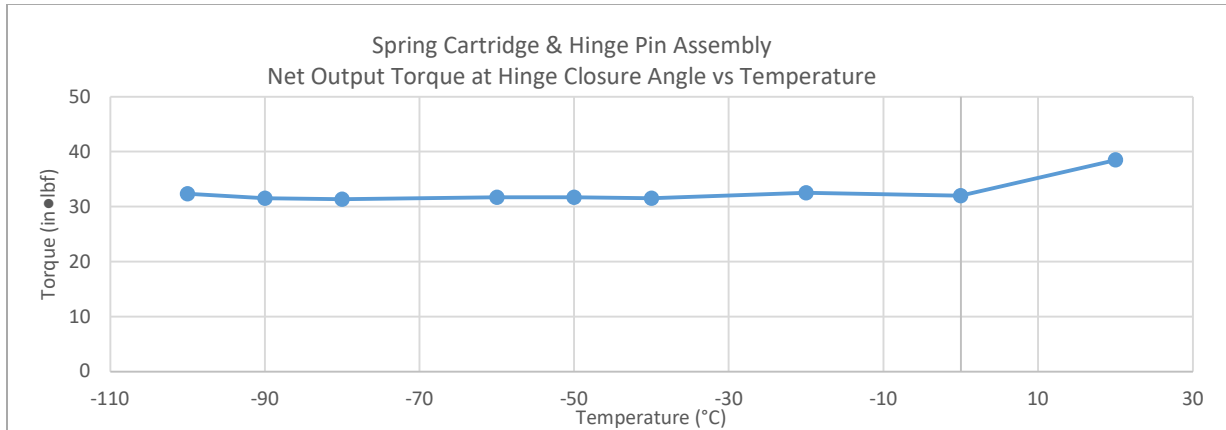


Figure 10. SWOT Mid-Hinge Spring Assembly Output Torque at Hinge Closure at Various Temperatures

### Rotary Viscous Damper Design Overview

Rotary viscous dampers have been used in dozens of spaceflight missions. Significant challenges have been encountered in the development and qualification of these dampers and several noteworthy breakthroughs in the design and assembly process including vacuum fluid degassing and fill methods and gasket sealing designs have been established as standard practice to ensure acceptably consistent performance and reliable operation in flight [2].

Building upon the state of the art rotary viscous damper baseline, JPL has partnered with D.E.B. Manufacturing Inc. to qualify an improved spring/piston rotary viscous damper design. The rotary viscous damper design used in this program is a variant of the heritage D.E.B. Manufacturing Inc. 1025 model damper. New design features include a higher strength Maraging 300 single wing vane shaft, updated custom ball bearing shields to reduce unintended leak paths from the damping chamber to the expansion chamber through the ball bearings, a more gradual taper on the valve adjustment surface for precision damping rate setting, an additional fastener holding the case and abutment together for added strength, and most notably a compression spring and gasketed piston arrangement to replace the heritage elastomeric diaphragm to pressurize the damping fluid expansion chamber as shown in Figure 11. Note this basic functionality of the spring/piston arrangement is similar to that of the spring/piston damper temperature compensator used on Mariner, Viking, Galileo, NSCAT and other missions [3].

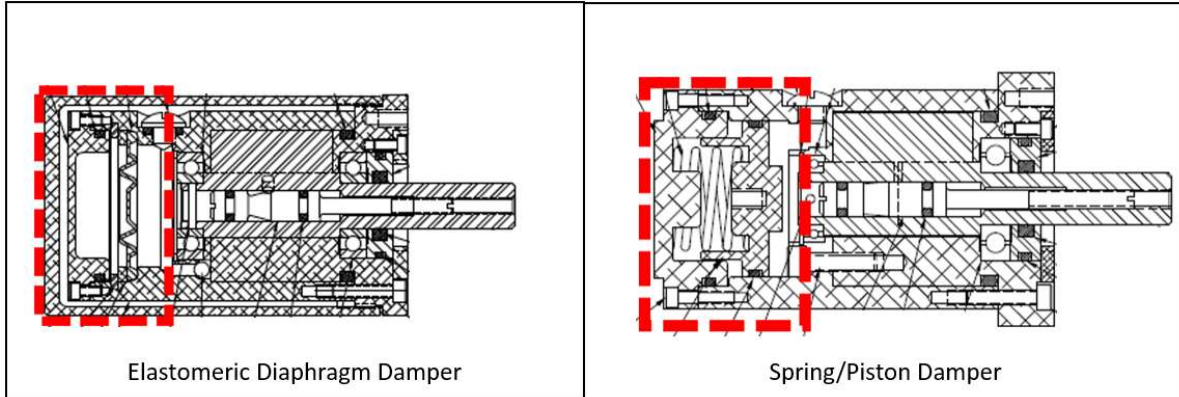


Figure 11: Heritage (Left) and New (Right) Viscous Dampers (Image Credit D.E.B. Manufacturing Inc.)

Initial prototype test results for this new D.E.B. Manufacturing Inc. damper design suggest several noteworthy performance advantages over heritage 1025 model dampers: reduced internal backlash, improved damping rate consistency, lower fluid recovery time, and greater structural robustness to transient impulse torque application (such as from deployable separation kickoff events). The sections that follow provide data supporting each of these observed advantages.

#### Empirical Data-Based Damper Analytical Model

As-tested damper performance for viscous dampers in this program did not conform well to ideal damper performance theory. This result is consistent with previous viscous damper characterization test program observations [3].

The ideal viscous damper is a rate-dependent torque device that conforms to the following simple equation:

$$T_{Damper} = c \cdot \dot{\theta} + T_{Coulomb} \quad (\text{Equation 1})$$

where 'c' is the damping rate constant, ' $\dot{\theta}$ ' is the angular velocity of the damper shaft, and ' $T_{Coulomb}$ ' is rate-independent friction torque loss of the damper. Damper testing demonstrates that the damping rate for any given device is not constant, varying significantly with both temperature and with applied torque. Data from prototype damper thermal testing was used to generate functions for damping rate verses applied torque at qualification temperature limits as well as the nominal expected flight deployment temperature. These curve-fit functions are shown in Figure 12.

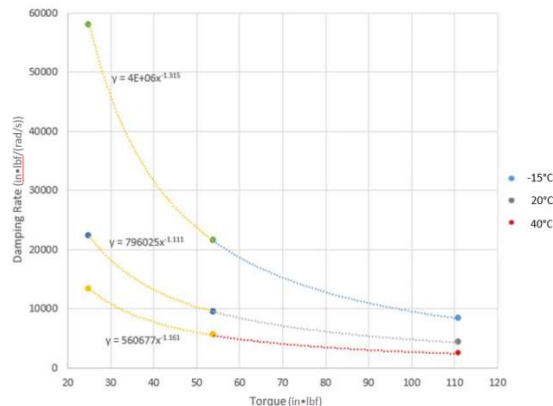


Figure 12. Measured Damping Rate vs Applied Torque at Different Temperatures

As shown in Figure 12, at a given applied torque, the damping rate varies by a factor of approximately four to five between qualification cold and qualification hot temperature extremes listed in Figure 12 for the low torque range shown. In order to comply with Project deployment duration requirement limits in all allowable flight thermal environments in spite of this significant damping rate variability with temperature, thermostatically-controlled film heaters have been added to the design baseline for all dampers on both the SWOT and NISAR spacecraft to actively control damper temperature.

Damper deployment simulations were conducted using this test-informed analytical model in order to calculate peak damper reaction loads and to generate preliminary deployment duration estimates for worst case flight environments and deployment configurations.

### Damper Variable Torque and Temperature Testing

In order to reduce risk of boom hinge deploy duration requirements non-compliances surfacing in the upcoming damper qualification program, prototype damper thermal testing was conducted with the highest and lowest net torque profiles applied to the damper throughout deployment at qualification temperature limits. Linearly decreasing torque was applied to the damper throughout the test using a chain-on-pulley configuration in which the chain piles on the floor, mimicking the near-linear reduction in torque available from flight deployment torsion springs. A linearly-decreasing maximum torque profile that bounds the worst-case flight torque profile was applied in the qualification hot temperature environment over the minimum hinge deploy angle to generate the shortest deployment duration result. Similarly, a linearly-decreasing minimum torque profile that bounds the worst case low flight torque profile was applied in the qualification cold temperature environment over the maximum hinge deploy angle to generate the longest deployment duration result. See test results in Figure 13.



Figure 13: Worst-Case Long (Left) and Worst-Case Short (Right) Deploy Duration Test Data

When these test results are compared to elastomeric diaphragm test results from past projects, the spring/piston damper exhibited more consistent damping rate performance under constant external torque application, as shown in Figure 14. The suspected explanation is that the spring recovers to achieve constant damping chamber pressure more quickly than the elastomeric diaphragm. Note there was a 9% difference in constant applied torque between the two plots shown below. While the lower applied torque in the spring/piston damper test may have influenced the damping rate consistency result, this is not expected to be a significant factor.

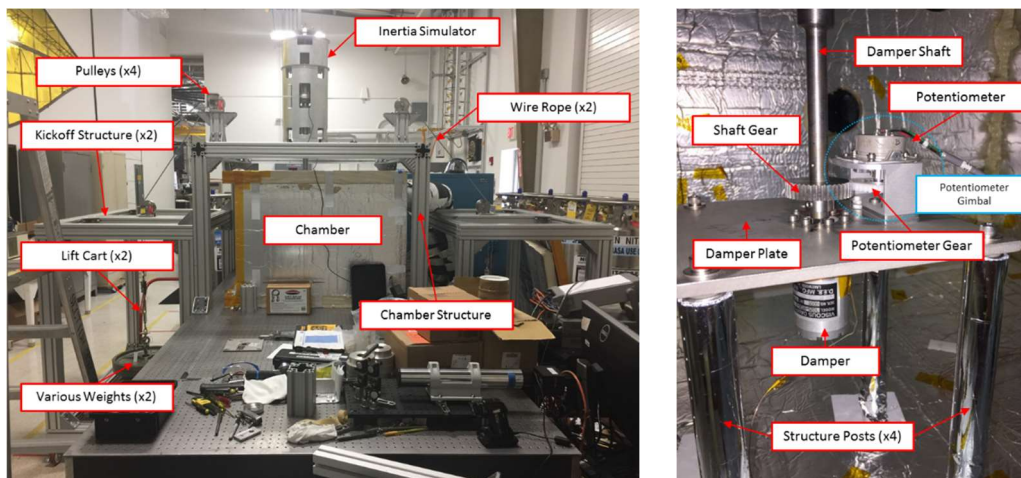


Figure 14: Comparison of Damping Performance with Constant Applied Torque

### Damper Impulse Torque Testing

At the time of SWOT and NISAR deployable boom launch restraint release, significant separation forces act on the boom from explicit kickoff springs as well as thermal-strain induced structural over constraint forces. These large forces are applied at the separation interfaces, which are a significant distance from the hinge lines. The result is high torque in excess of 678 N•m (6,000 in•lbf) applied about the hinge line. The damper is intentionally isolated from this torque with rotational backlash in the torque transmission hardware and by pre-setting the damper shaft rotation angle to the “backseat” of this backlash prior to launch.

A damper kickoff simulation test was implemented to represent this critical load case as shown in Figure 15. The maximum achievable kickoff torque for the test setup was implemented at approximately 775 N•m (6858 in•lbf), applied over the full stroke angle of the mast separation kickoff spring plungers. This peak torque was applied to rotational inertia simulators that bounded the relevant inertia of the flight hinges. Flight-like damper torque transmission backlash was represented in the test. Damper temperature was controlled to the extremes of the qualification temperature range, and damper torque response was measured (see Figure 15). Average damping rate over this brief duration was calculated and used to generate functions for damping rate verses applied torque in the high torque regime (see Analytical Modeling section).



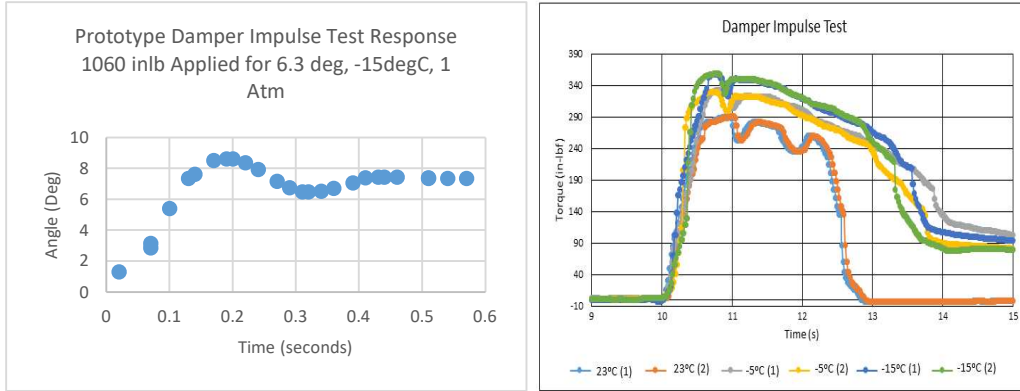


Figure 15. Prototype Damper Impulse Torque Test

The plot in Figure 16 shows significant initial damper backlash from the heritage elastomeric diaphragm damper design with significantly lower nominal damping rate of 101.7 N•m/(rad/s) (900 in•lbf/(rad/s)) versus 565 N•m/(rad/s) (5000 in•lbf/(rad/s)) with the current design. No damper backlash has been observed in prototype testing of the spring/piston damper.

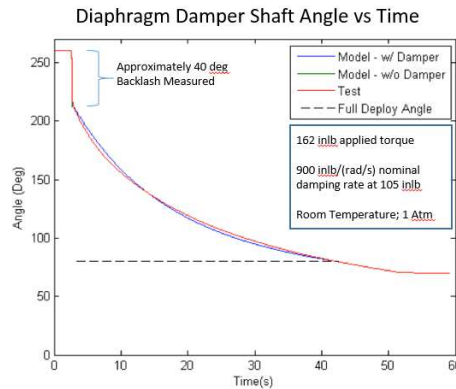


Figure 16. SMAP Project Damper Test Data Showing Typical Diaphragm Viscous Damper Backlash

With high enough torque applied, D.E.B. Manufacturing Inc. reported they have permanently deformed the elastomeric diaphragm in test dampers, resulting in cavitation issues and in some cases external gas entrainment into the expansion chamber and damping chamber (see Figure 17). Prototype high-torque impulse testing of the spring/piston damper has demonstrated the robustness of this design against catastrophic damage due to short duration high torque events, as can be generated by kickoff springs and strain energy in flight deployable separations. The elastomeric diaphragm can also permanently deform from hot and cold temperature deployments and thermal vacuum cycling. The spring/piston damper also reduces the list of non-metallic, permeable materials within the damper to only gaskets and O-rings, reducing the potential for unintended fluid seepage through the diaphragm (also reported by D.E.B Manufacturing Inc. in testing).

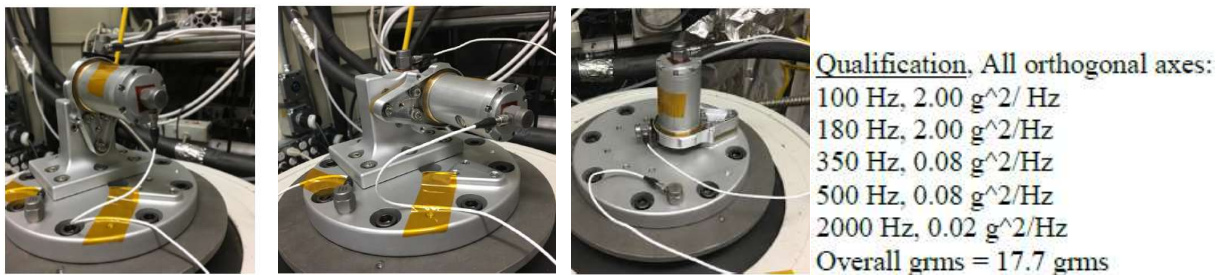


Figure 17: New Diaphragm (Left) and Inelastically Deformed Test Diaphragm (Right)

Due to intermittent issues with cavitation and prolonged recovery time in developmental testing for the Soil Moisture Active Passive (SMAP) Project with the elastomeric diaphragm damper, the SMAP Project instituted a two hour wait for damping fluid recovery prior to subsequent damper usage. Prototype testing with the spring/piston damper has demonstrated that 30 minutes is adequate recovery time (note: less time may be acceptable but has not been tested). The slow process of the elastomeric diaphragm recovering its original shape is the suspected root cause of the prolonged recovery time for the elastomeric diaphragm damper. It is important to note the elastomeric diaphragm may never recover to its original shape and can be permanently deformed resulting in cavitation issues and in some cases external gas entrainment into the expansion chamber and damping chamber.

### Damper Vibe Testing

In the SWOT and NISAR deployable reflector boom mechanism, the damper shaft must be mechanically isolated from the high kickoff torque of the boom. These high torques are applied to the boom over a maximum angle of 0.8 degrees. In the ground stowing process, the damper shaft is positioned in the “backseat” of the 4 degree minimum backlash. It is critical that the shaft not rotate within this backlash in the launch vibe environment. To demonstrate that the damper shaft does not move in a bounding vibratory environment simulating launch vibe, a random vibration test was conducted with the damper mounted on its flight-like mounting bracket. Tests were conducted in 3 orthogonal axes as shown in Figure 18. The initial damper shaft clocking was marked on the housing. It was confirmed that the shaft did not rotate from the initial clocking after each 2.5 minute test. Test levels are shown in Figure 18.



*Figure 18. Damper Vibration Test (X-, Y-, & Z-Axes from Left to Right)*

### **Hinge Latching Mechanism**

The hinge latching mechanism preloads precision alignment features on each hinge half to each other after hinge closure. There is a separate latching mechanism located at each hinge. Each latching mechanism consists of an actuator with torque transmission hardware, and a flexured hook/roller assembly (see Figure 19). Noteworthy design, analysis, and test information for each of these are described in the sections that follow.

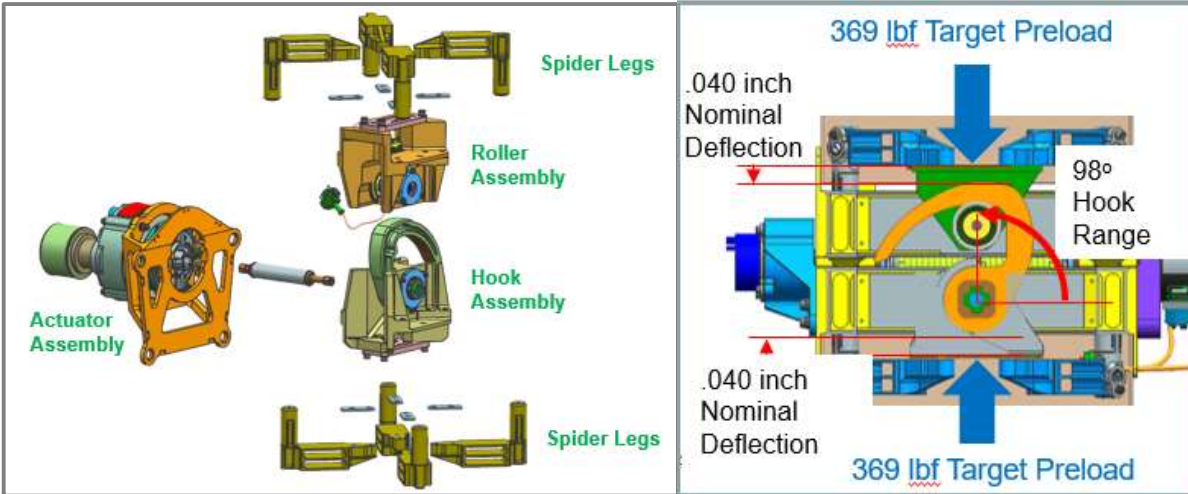


Figure 19. Hinge Latching Hardware Overview

### Latching Actuator Thermal Testing

The harmonic gear set used in the actuator is not capable of transmitting more than 22.6 N•m (200 in•lbf) of torque without ratcheting gear teeth. Stall torque was adjusted to just below this threshold in the worst case hot (highest output torque) environment for actuator operation. A significant reduction in actuator output torque of about 43% was observed in prototype testing from this maximum at the worst-case hot environment (75°C) to the worst-case cold environment (-30°C) due to Braycote 601 lubricant thickening and reduction in motor winding resistance at cold temperature as shown in Figure 20. This reduced output torque performance in the worst case cold environment drives the minimum latching mechanism torque margin.

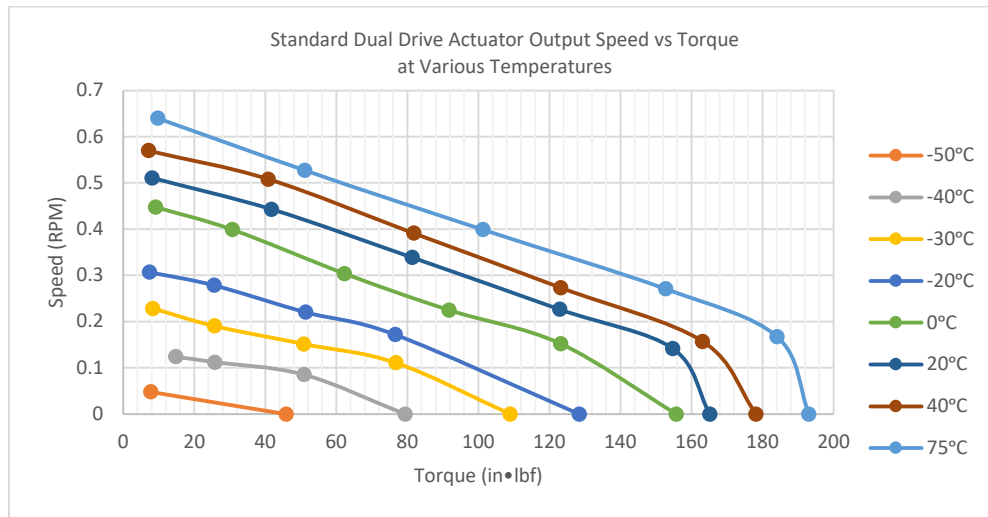


Figure 20. Actuator Speed versus Torque Performance at Various Temperatures

Dynamometer testing of a prototype actuator demonstrated a slight improvement in actuator output torque performance in the worst case cold condition by adding a few drops of Brayoil 815Z to the Braycote 601 grease on the internal motor ball bearings when compared to the same bearings with only Braycote 601 added (see Figure 21). This lubrication approach is being used for both the SWOT and NISAR Projects.

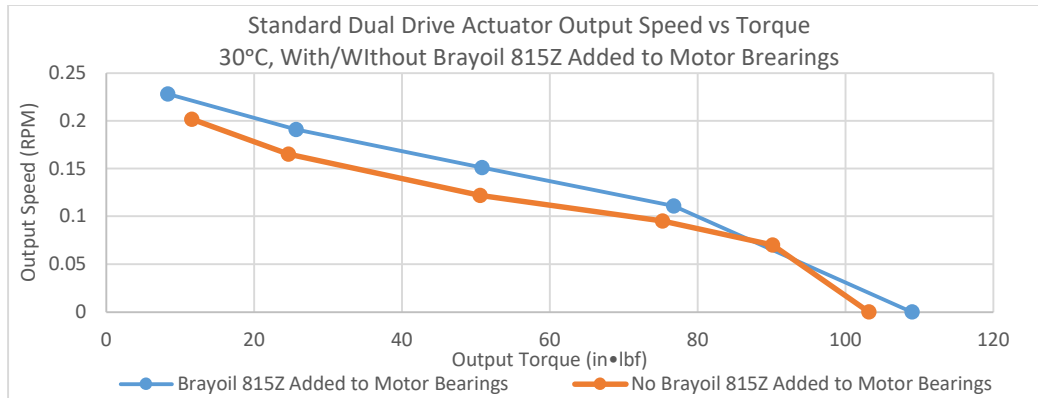


Figure 21. Actuator Performance with and without Brayoil 815Z Added to Braycote 601 on Motor Bearings

### Flexured Hook and Roller Assembly

The flexured hook and roller assembly is designed to achieve the target joint preload of 1641 N (369 lbf) while requiring the minimum peak torque to latch within available volume constraints. A modified parabolic hook ramp profile was designed to maintain nearly constant torque required during the latching process, minimizing peak torque required to approximately 5.65 N•m (50 in•lbf) and thereby maximizing mechanism minimum torque margin.

The significant deflection of the flexures in the assembly of approximately 2.03 mm (.080 in) under preload ensures that there is not significant change in preload due to mismatch in the coefficients of thermal expansion between latch component materials and alignment critical structure materials. A three-blade one-axis flexure was designed to achieve the required stiffness and stroke in the limited volume available.

### **Conclusions**

The following key mechanism conclusions have been drawn based on the NISAR and SWOT RF Boom Hinge deploy and latch mechanism developmental testing and analysis results referenced in this document:

1. Mechanical decoupling of mechanism hardware from alignment critical structures is a simple, robust and effective approach to avoidance of mechanism-induced thermal distortions
2. High aspect ratio rectangular wire torsion spring arms must be adequately supported to prevent undesirable twist along the wire axis when used at significant angles of deflection.
3. The new spring/piston viscous damper design described in this document provides performance benefits over heritage elastomeric diaphragm dampers.
4. The addition of Brayoil 815Z to Braycote 601 lubricant provides measurable improvement in cold temperature ball bearing performance.

### **References**

1. NASA-STD-5017A, "Design and Development Requirements for Mechanisms", 2015-7-31, 62.
2. Stewart, Alphonso, Charles Powers, and Ron Lyons. "Improvements for Rotary Viscous Dampers Used in Spacecraft Deployment Mechanisms." Proceedings of the 32<sup>nd</sup> Aerospace Mechanism Symposium, 115-124.
3. Harper, Jack. "Viscous Rotary Vane Actuator/Damper." Proceedings of the 10<sup>th</sup> Aerospace Mechanisms Symposium, 198-207.

### **Acknowledgement**

The research described above was carried out at the Jet Propulsion Laboratory, California Institute of Technology and at D.E.B. Manufacturing, Inc. under a contract with the National Aeronautics and Space Administration